Hindawi
Canadian Journal of Infectious Diseases and Medical Microbiology
Volume 2023, Article ID 4627848, 15 pages
https://doi.org/10.1155/2023/4627848

Research Article

Anti-Biofilm Effect of Ampicillin-Loaded Poly (Lactic-co-glycolic Acid) Nanoparticles Conjugated with Lysostaphin on Methicillin-Resistant *Staphylococcus aureus*

Elahe Norouzi,[1] **Seyed Mostafa Hosseini**,[1] **Babak Asghari**,[1] **Reza Mahjoub**,[2] **Ehsan Nazarzadeh Zare**,[3] **Mohammad-Ali Shahbazi**,[4] **Fereshte Kalhori**,[5] **and Mohammad Reza Arabestani**[1,6]

[1]*Department of Microbiology, Faculty of Medicine, Hamadan University of Medical Sciences, Hamadan, Iran*
[2]*Department of Pharmacology and Toxicology, School of Pharmacy, Medicinal Plants and Natural Products Research Center, Hamadan University of Medical Sciences, Hamadan, Iran*
[3]*School of Chemistry, Damghan University, Damghan, Iran*
[4]*Department of Biomedical Engineering, University Medical Center Groningen, University of Groningen, Antonius Deusinglaan 1, 9713 AV Groningen, Netherlands*
[5]*Biotechnology Department, Hamadan University of Medical Sciences, Hamadan, Iran*
[6]*Infectious Disease Research Center, Hamadan University of Medical Sciences, Hamadan, Iran*

Correspondence should be addressed to Mohammad Reza Arabestani; mohammad.arabestani@gmail.com

Received 18 June 2023; Revised 7 November 2023; Accepted 27 November 2023; Published 6 December 2023

Academic Editor: Vijay Gondil

Staphylococcus aureus exhibits the capacity to develop biofilms on various surfaces, encompassing both living and nonliving substrates, enabling it to develop resistance against the immune system and antibiotics. Therefore, this bacterium can cause numerous challenges in healthcare and treatment systems. The present study aimed to investigate the ampicillin-loaded PLGA nanoparticles' effect on preventing the methicillin-resistant *Staphylococcus aureus* (MRSA) biofilm formation when it is conjugated with lysostaphin. With the use of the double emulsion evaporation technique, nanodrug carriers were created. Physicochemical attributes of the nanoparticles, such as particle size, drug loading, PDI, encapsulation efficiency, zeta potential, efficiency of lysostaphin conjugation, and morphology, were measured. Minimum inhibitory concentration (MIC), well diffusion, and other techniques were used to investigate the effect of the produced nanodrug carrier on strains of *S. aureus*. A toxicity test was conducted to examine the toxic effects of artificially generated nanomedicines on the L929 fibroblast culture. The nanoparticle average size, zeta potential, PDI, lysostaphin conjugation efficiency and drug loading encapsulation efficiency, and in the optimum PLGA-AMP-LYS (F4) formulation were 301.9 ± 32 nm, 0.261 ± 0.010, -19.2 ± 3.4 mV, 18.916 ± 1.6, and 94.53 ± 3.8, 40%, respectively. After 72 hours, neither the well diffusion nor MIC techniques revealed any discernible variation between ampicillin and nanodrug carriers. The biofilm investigation's findings, however, indicated that compared to the free drug, the hindering effect of the nanodrug carrier was greater after 72 hours. The toxicity test findings revealed that the synthesized nanodrug had no toxic effects on the cells. Given the excellent efficacy of the nanomedicine carrier established in the present study, applying this technology to combat hospital-acquired infections caused by Staphylococcus bacteria could yield significant benefits in managing staphylococcal infections.

1. Introduction

Given the lengthy and expensive nature of developing new drugs, repurposing existing drugs is becoming increasingly popular. Additionally, strategies that aim to enhance the effectiveness of antimicrobial treatments can contribute to reducing drug resistance. Extensive research has been conducted on nanoparticles as promising drug carriers, given their capacity to improve the infiltration of antimicrobial drugs into the biofilms' deeper layers. Leveraging

nanoparticles to elevate the medicinal properties of currently available antibiotics shows great potential as a viable strategy [1]. Nanoparticles facilitate the improved delivery of antimicrobial medications to the dense biofilm layers [2]. Nanoparticle-based drug carriers protect the enclosed medication against various factors, including enzymatic and chemical degradation [3, 4]. Drug release from nanoparticles is continuous and controlled, and drug spreads in biofilm layers [5]. PLGA has gained significant attention among the numerous nanoparticles due to its remarkable biocompatibility, biodegradability, absence of toxicity, approval from the European Medicine Agency and the Food and Drug Administration (FDA), controlled and stable drug release, targeted delivery to specific cells or organs, as well as its compatibility with a wide range of hydrophilic and hydrophobic drugs [6–8]. The polymerization of lactic and glycolic acid monomers forms a copolymer which is PLGA. The improved treatment effect and the accelerated healing process are results of the controlled and stable drug release from PLGA [5]. The use of bacteriocins is another biofilm treatment method. Antimicrobial peptides called bacteriocins are useful for treating infections caused by biofilms [9]. Staphylococcins are a group of bacteriocins that have been identified from several Staphylococcus species, collectively known as staphylococcins. Staphylococcins, including aureocin 53, epidermin, pep5, and lysostaphin, are active against all staphylococcus species [9]. 246 amino acids make up the 27 kDa zinc metalloenzyme known as lysostaphin, which is very active against *Staphylococcus aureus* strains. In 1964, Schindler and Schuhardt isolated lysostaphin from Staphylococcus simulans biovar staphylolyticus [10]. *Streptococcus aureus* strains' cell walls contain pentaglycine bridges that are broken by this enzyme [10, 11]. Ampicillin, which belongs to the aminopenicillin family, is a beta-lactam antibiotic that is generally comparable to its successor, amoxicillin, in terms of spectrum and level of activity [12]. Following the introduction of ampicillin, a significant number of bacteria have developed resistance to it by producing beta-lactamases [13]. *S. aureus* is an opportunistic and life-threatening Gram-positive pathogen. It is recognized as a contributor to both healthcare-associated infections and community-acquired infections, encompassing minor skin conditions to severe ailments such as sepsis, pneumonia, and endocarditis. Moreover, this particular bacterium is renowned for being a common reason behind the infections of soft tissue and skin [14, 15]. Since the 1980s, methicillin-resistant *Staphylococcus aureus* (MRSA) has spread worldwide, reaching a point where many countries now observe MRSA rates of 50% or higher among *Staphylococcus aureus* infections in hospitals. However, a few countries have managed to maintain low MRSA rates by implementing effective search-and-destroy policies and controlling antibiotic overuse [16]. *Staphylococcus aureus* colonization is in two forms: persistent carriers (20–25%) and intermittent carriers (75–80%), which shows a clear correlation between the risk of hospital infections and *S. aureus* nasal carriers [17]. *S. aureus* strains have two modes with different characteristics: planktonic state and biofilm state [18]. Bacteria are encased within a self-generated extracellular polymeric matrix when in the biofilm state [19]. The biofilm matrix mainly consists of exopolysaccharides, eDNA, and proteins protecting bacteria against various environmental stresses [17, 20]. Biofilm formation includes different steps: first, planktonic bacteria reversibly attach to biotic or abiotic surfaces. The attachment becomes irreversible. Next, microcolonies form and then mature. Finally, the biofilm disperses, and the planktonic cells are released from the biofilm. The planktonic cells are attached to other areas, and biofilm is formed again. Therefore, biofilm-related infections are often chronic and recurrent [17, 20]. In addition, infections associated with biofilms display resilience against the majority of antibiotics and the immune system of the host [1, 20]. Getting infected in venous ulcers, and pressure sores, and developing diabetic foot conditions are associated with the existence of Staphylococcus aureus capable of producing biofilms. Among the different drug-resistant strains of *Staphylococcus aureus*, hospitalized patients with wound infections face a substantial risk from methicillin-resistant Staphylococcus aureus (MRSA). Strains of MRSA that generate biofilms lead to illness and fatalities in humans [21]. Increasing the dosage of antibiotics and extending the duration of infection treatment is necessary to combat bacterial biofilms, albeit resulting in elevated resistance and side effects. [22]. Furthermore, sessile cells display unique features in contrast to their planktonic counterparts, which can potentially result in elevated antibiotics' minimum bactericidal concentration (MBC) and minimum inhibitory concentration (MIC) values [1, 20]. Therefore, how should these infections be treated remains a challenging question, and innovative strategies are needed to eradicate bacterial biofilm-related infections [23]. Utilizing nanoparticles for the targeted delivery of antibiotics to the biofilm's interior layers is considered a promising strategy [24]. Using nanoparticles prolongs bacterial exposure to antibiotics by enabling sustained and controlled drug release, thereby reducing the necessity of dosage escalation [5]. Thus, in this research, the impact of poly (lactic-co-glycolic acid) polymer nanoparticles loaded with ampicillin and linked with lysostaphin on the inhibition of MRSA biofilm was investigated *in vitro*.

2. Materials and Methods

2.1. Materials. Ampicillin, polyvinyl alcohol (PVA), poly (lactic-co-glycolic acid) (PLGA) 50 : 50 (30,000–60,000 g/mol), and lysostaphin were acquired from Sigma Aldrich (MO, USA). The N-hydroxysulfosuccinimide (NHS), 1-ethyl-3-(3-dimethylaminopropyl) carbodiimide hydrochloride (EDC), and 2-morpholinoethanesulfonic acid (MES) were also supplied by Sigma Aldrich (MO, USA). Two assay kits, including the MTT and the Bradford protein assay kit, were produced in Kiazist, Iran. The Mueller–Hinton agar, blood agar, Mueller–Hinton broth, dichloromethane, and chloroform were purchased from Merck (Darmstadt, Germany). Fetal bovine serum (FBS), penicillin, and streptomycin were obtained from Gibco in the United States. Additionally, Dulbecco's modified Eagle's medium (DMEM) was employed.

2.2. PLGA-AMP Synthesis. The PLGA-AMP was fabricated using the double emulsion-solvent evaporation method. Briefly, a total of 120 mg of PLGA polymer was dissolved in 15 mL of chloroform and agitated on a magnetic stirrer at 25°C and 150 rpm for a duration of 3 hours. After that, 24 mg of ampicillin was added to the mixture, and the first emulsion (W1/O) was formed. The previously dissolved PVA powder in distilled water (PVA 2%) was added to the first emulsion, and the secondary emulsion was formed (W1/O/W2). The sample was then subjected to homogenization by employing an ultrasonic probe device (Bandelin Sonopuls, Berlin, Germany) operating at 45% amplitude (20 W) for a duration of two minutes, following a consistent pulse pattern of 10 seconds on and 5 seconds off. Dropwise additions of the second emulsion were made with magnetic stirring for 30 minutes in 20 mL of cold distilled water (4°C). By employing a high-speed centrifuge (37,000 g for 20 minutes), PLGA-AMP was finally separated [25]. Lyophilization of the prepared samples was performed at −80°C with a vacuum pump (Christ, China) equipped with a condenser flow system. The lyophilized nanoparticles were converted into a solution and then sterilized using 450 nm filters to make them appropriate for biological research involving bacteria and cell lines.

2.3. Lysostaphin Conjugation. A total of 20 mg of PLGA-AMP NPs were dispersed in 10 mL of MES buffer (pH 5.0) according to Moura et al. protocol [26]. The activation process involved the addition of 1 mL of 0.1 M EDC and 1 mL of 0.7 M NHS to the nanoparticle suspension. The suspension was allowed to stand at room temperature while being gently stirred for a duration of 1 hour. In order to remove any remaining reagents, the activated nanoparticles were centrifuged at 21,000 g for 10 minutes at 4°C and subsequently redispersed in phosphate-buffered saline (PBS). Next, 3 mg of lysostaphin was added to the NP suspension, followed by homogenization using a vortex mixer. The resulting suspension was incubated at 4°C for 24 hours. A second round of centrifugation was achieved to eliminate any conjugated lysostaphin. The pellets obtained were redissolved in PBS. To assess the effectiveness of lysostaphin conjugation to PLGA-AMP nanoparticles, the Bradford protein assay was performed using the Coomassie Plus (Bradford) kit [26].

2.4. Characteristics of NPs. The particle size, PDI (Polydispersity Index), and Zeta potential were measured following the lyophilization process using the Dynamic Light Scattering (DLS) technique and the Zetasizer Nano ZS 3600 equipment from Malvern Devices in Worcestershire, in the UK [27].

2.5. Morphology. The morphological characteristics of the nanoparticles were analyzed using Field Emission Scanning Electron Microscopy (FE-SEM). In summary, a mixture of 1 mL of distilled water and 10 mg of lyophilized PLGA-AMP nanoparticles was prepared, and then 2 μL of this mixture was deposited onto a glass surface. To prevent electrostatic charge during examination and analysis using FE-SEM (TSCAN, Czech Republic), a thin gold layer was applied to the dried suspension [28].

2.6. Determination of Entrapment Efficiency (EE %) and Drug Loading (DL %). Following guidelines from the literature, an indirect method involving a spectrophotometer was employed to ascertain the amount of ampicillin loaded and encapsulated within the synthesized nanoparticles. Initially, 1 mL of distilled water was combined with 5 mg of lyophilized nanoparticles, and the mixture was vortexed. The subsequent step involved centrifugation at 37,000 g for 20 minutes at 4°C. A 268 nm-wavelength spectrophotometer (2100UV, USA) was used to analyze the supernatant. The drug's concentration was found using a standard curve. The amount of drug that was loaded (equation-(2)) and encapsulated (equation-(1)) was calculated using the following equations [29, 30]:

$$\text{Entrapment Efficiency EE (\%)} = \frac{\text{initial drug amount (24 mg)} - \text{free drug amount (1.3 mg)}}{\text{initial drug amount (24 mg)}} \times 100 = 94.5, \quad (1)$$

$$\text{Drug Loading DL (\%)} = \frac{\text{initial drug amount (24 mg)} - \text{free drug amount (1.3 mg)}}{\text{initial PLGA amount (120 mg)}} \times 100 = 18.91. \quad (2)$$

2.7. Determination of Stability of NPs. The nanoparticles' stability was monitored at periodic intervals of time. Using nano Zetasizer devices, the stability of NPs was evaluated by measuring their particle size, zeta potential, and PDI at intervals of 0, 2, 4, 6, 8, and 12 months after the process of lyophilization. A spectrophotometer was used concurrently to determine the quantity of ampicillin encapsulated in the nanoparticles [31].

2.8. Determining Drug Release. After carefully weighing the lyophilized nanoparticles, they were added to a 40 ml release medium (PBS buffer, pH: 7.4) within a dialysis bag (12,000 Da molecular weight cut-off, sourced from Dialysis tubing, Sigma Chemical Co., Missouri, USA). The system was simultaneously stirred with a magnetic stirrer at 100 rpm as 37°C temperature was maintained. One mL of the medium was taken at regular intervals, and the ampicillin content was measured using a spectrophotometer. A similar technique was carried out with free ampicillin placed in the same medium and encased in the dialysis bags in order to contrast this set of tests' outcomes with those of free ampicillin. Then, numerous samples were collected from the medium during the same time, and they were examined. It is important to highlight that after each withdrawal of a sample from the medium, a similar amount of fresh medium was promptly replenished [32].

2.9. The Differential Scanning Calorimetry (DSC) and Fourier-Transform Infrared Spectroscopy (FTIR). To scrutinize any possible interactions between the components in PLGA-AMP nanoparticles and ampicillin, a series of tests were conducted. This aspect was explored through FTIR analysis within the temperature range of 400 to 4000°C. DSC analysis was also performed in the temperature range of 20 to 400°C at a rate of 10°C per minute to confirm the drug loading in the PLGA matrix [33, 34].

2.10. MTT Assay. For assessing cytotoxic effects, a murine fibroblast cell line was employed to conduct the MTT assay on PLGA-AMP, free-AMP, lysostaphin, and pure PLGA. The kit contained a 96-well clean plate, two-channel reservoirs, solvent, and MTT reagent. In this procedure, 104 L929 fibroblasts were isolated using trypan blue staining, and then they were placed into 96-well cell culture plates filled with DMEM medium containing 10% FBS (fetal bovine serum) and 1% penicillin-streptomycin. Subsequently, the cells were cultured overnight at 37°C with 5% CO2. Following the removal of the DMEM culture medium, PLGA-AMP, free-AMP, lysostaphin, and pure PLGA were introduced into the cell culture, along with DMEM containing 10% FBS, and were then incubated for 24 hours. The concentrations used were 25 μg/mL, 50 μg/mL, 100 μg/mL, and 200 μg/mL. Positive controls consisted of wells containing the culture medium but no drug. Each experiment was conducted three times. Following the addition of 150 μL of fresh DMEM without fetal bovine serum to each well, all cells were washed with PBS to eliminate any residual drugs and polymers. Then, 20 μL of the MTT assay reagent was placed into every well. For three to four hours, the plate underwent incubation at 37°C with 5% CO2. To dissolve formazan particles, a 100 μL solubilizer was then added to each well and well mixed for 15 min, using an orbital shaker. The absorbance at 570 nm was measured with a 96-well ELISA plate reader. The extent of the positive charge's absorption became the main factor used to establish the viability of cells [35].

2.11. Bacterial Strains. Methicillin-resistant *Staphylococcus aureus* (MRSA) (ATCC 33591) and methicillin-sensitive *Staphylococcus aureus* (MSSA) (ATCC 25923) were the bacterial strains chosen for this study. Besides, the clinical strain was isolated from Besat Hospital, Hamadan, Iran.

2.12. Minimum Inhibitory Concentration (MIC) and Agar Well Diffusion. According to CLSI recommendations, agar well diffusion and minimum inhibitory concentrations (MIC) tests were conducted. In each well, 100 μL of PLGA-AMP, PLGA-AMP-LYS, and free-AMP were administered at varying concentrations (5, 25, and 50 μg/mL) and incubated for 24, 48, and 72 hours at 37°C. Subsequently, the diameter of the inhibitory zone was measured for each well. Additionally, the MIC test was conducted using sterilized 96-well cell culture plates. PLGA-AMP, PLGA-AMP-LYS, and free-AMP were dispensed at various concentrations, with 100 μL of each concentration added to individual microplate wells, excluding the control wells. In each well, 100 μL of Muller–Hinton broth medium was introduced, and subsequently, 100 μL of different bacterial strains at a concentration of $1.5 \times 10\hat{}6$ CFU/mL were added, except for the control well. For 24, 48, and 72 hours, the microplates were incubated at 37°C in an incubator [36, 37].

2.13. Analysis of Biofilm Inhibition. For the quantitative evaluation of forming biofilms with and without nanoparticles and free drugs, the crystal violet staining method was employed. To put it briefly, newly cultured strains were thinned out at a 1 : 100 ratio and incorporated into the TSB culture medium enriched with a 1% glucose solution. The final concentration of each microplate well was 50, 30, 20, 10, or 5 μg/mL. After that, various quantities of PLGA-AMP, PLGA-AMP-LYS, and free-AMP were employed. The microplate underwent 24, 48, and 72 hours of incubation at 37°C. The culture medium in each well was subsequently aspirated, and the wells were washed three times with PBS. Methanol was employed to fix the biofilm within each well. Subsequently, the wells were stained with a 2% crystal violet solution. After a 15-minute staining period, the wells were gently rinsed with water. The next step involved creating a suspension of adherent cells in 95% ethyl alcohol. Subsequently, the optical density (OD) was evaluated at 600 nm after a 30-minute incubation period [38].

2.14. Statistical Analysis. Statistical analysis was performed using ANOVA to assess the differences among the treatments. Another statistical method utilized to compare the groups was the Dunnett test. A 95% confidence interval was established, and statistical significance was defined as $P < 0.05$.

3. Results

3.1. The NPs' Properties. In the optimal PLGA-AMP-LYS formulation (F4), the nanoparticles exhibited a mean diameter of 301.9 ± 32 nm, a PDI of 0.261 ± 0.010, and a zeta potential of -19.2 ± 3.4 mV, as shown in Table 1.

Table 1: Components and technological parameters of various formulations.

Formulation	AMP (mg)	LYS (mg)	PLGA (mg)	DCM[1] (ml)	Chl[2] (ml)	PVA (ml)	Size (nm)	PDI	ZP (mV)	EE (%)	DL (%)	LCE[3] (%)
F1	6	—	30	20	—	20 (1%)	724.4 ± 45	0.372 ± 0.021	−18.5 ± 1.6	92.24 ± 7.3	13.91 ± 1.2	—
F2	6	—	30	—	15	20 (1%)	435.4 ± 23	0.280 ± 0.014	−17.3 ± 1.5	93.43 ± 5.2	15.53 ± 1.4	—
F3	12	—	60	—	15	20 (2%)	321.2 ± 36	0.274 ± 0.012	−20.5 ± 2.1	93.50 ± 4.5	16.42 ± 2.3	—
F4	**24**	**3**	**120**	—	**15**	**20 (2%)**	**301.9 ± 32**	**0.261 ± 0.010**	**−19.2 ± 3.4**	**94.53 ± 3.8**	**18.91 ± 1.6**	**40**

[1]Dichloromethane. [2]Chloroform. [3]Lysostaphin conjugation efficiency. Bold values represent the best formulation used in the study.

3.2. Morphology. The outcomes of PLGA-AMP morphology analysis via FE-SEM are shown in supplementary file 1. Based on the image, the majority of the particles appeared to be spherical, displaying a smooth surface and exhibiting a uniform dispersion. The size and PDI (0.261 ± 0.010) of most nanoparticles were consistent with this observation.

3.3. Drug Loading and Encapsulation Efficiency. The range for the quantity of ampicillin loaded in PLGA in various formulations was 13.91% to 18.91%, while the range for the amount of encapsulation was 92.24% to 94.53%. In the optimized PLGA-AMP-LYS (F4) formulation, the levels of ampicillin loaded and encapsulated were $18.91\% \pm 1.6$ and $94.53\% \pm 3.8$, respectively, as depicted in Table 1.

3.4. Stability of NPs. The nanoparticles' zeta potential, PDI, and particle size were evaluated at intervals of 0, 2, 4, 6, 8, and 12 months after production (Table 2). The findings indicated that at least till the sixth month after production, there was very little variation in the size of the nanoparticles. These diameters went from 301.9 ± 32 nm to 502.6 ± 43 nm after a year. Zeta potential and PDI changes were not appreciably different.

3.5. Drug Release. The drug release test was conducted over 72 hours in an in vitro setting using a PBS buffer with a pH of 7.4. The findings are displayed in Figure 1. Results showed that the time required was more than 72 hours to release approximately 80% of the drug from the PLGA matrix. In comparison, 80% of the free drug was released within the initial 30 hours, and within the first 20 hours, 35% of the drug was released from the PLGA matrix. During this same time frame, 75% of the free drug was released.

3.6. FTIR Analysis. The FTIR spectra of ampicillin, PLGA, and PLGA-AMP are displayed in Figure 2. Encapsulating ampicillin in PLGA nanoparticles prevents the drug's absorption peaks at 985 cm^{-1}, as can be seen in this figure. However, inside the same sites of PLGA-AMP, three ampicillin feature absorption peaks are seen at 1450 and 985 cm^{-1}. When PLGA and PLGA-AMP nanoparticle spectra are compared, it can be seen that the PLGA-AMP nanoparticle spectra appear to have strong PLGA absorption peaks at 2980 and 1500 cm^{-1}.

3.7. DSC Analysis. To scrutinize PLGA nanoparticles' recrystallization and melting characteristics, we acquired DSC thermograms for ampicillin, PLGA, a physical mixture, and PLGA-AMP nanoparticles (Figure 3). The DSC thermogram for PLGA illustrates a melting transition at a temperature of 200°C. Remarkably, the melting points of both the physical mixture and the nanoparticles closely resembled those of the PLGA. During the physical blending with ampicillin, a subtle alteration in the melting behavior of PLGA was detected. The DSC thermograms of ampicillin showed a clear endothermic peak, manifesting at a temperature of 220°C. The melting points of both the physical mixture and PLGA-AMP nanoparticles appear relatively low in comparison to data regarding this characteristic for other substances. Of particular significance is that there was little to no change in the physical mixture, PLGA-AMP, or endothermic peak positions of the ampicillin. The absence of a discernible melting peak in the PLGA-AMP thermogram indicates that the ampicillin molecules are potentially stabilized within the PLGA matrix or that there is an absence of freely present ampicillin crystals within the PLGA-AMP structure.

3.8. MTT Assay. The toxicity evaluation of murine L929 fibroblasts exposed to varying concentrations of PLGA-AMP, ampicillin, free PLGA, and lysostaphin can be observed in Figure 4. At 37°C and 5% CO2, cells were cultivated with varying concentrations of free ampicillin, PLGA-AMP, free PLGA (blank), and lysostaphin. Furthermore, the identical cells employed in the positive control group (untreated) were subjected to incubation in the culture medium. All formulations had no toxic effect to 50 μg/ml. The toxicity of PLGA-AMP was lower than free ampicillin at 200 μg/ml.

3.9. Agar Well Diffusion and Minimum Inhibitory Concentration (MIC). Tables 3 and 4 display the well diffusion and MIC test results at 24, 48, and 72 hours. Free ampicillin had a better impact on all three strains in both techniques at 24 and 48 h than PLGA-AMP. The anticipated results can be attributed to the fact that, in both approaches, the bacteria were exposed to the freely available drug; however, only a minimal quantity of the medication was released from the PLGA-AMP. In addition, the release of medication from PLGA-AMP occurred after 72 hours of incubation, which gradually increased the inhibition zone of PLGA-AMP. The MIC of PLGA-AMP also approached that of free ampicillin after 72 hours. Lysostaphin-conjugated nanoparticles had no inhibitory effect on *Staphylococcus aureus* strains at 24, 48, and 72 hours after incubation.

3.10. Biofilm Analysis. The results pertaining to the impacts of PLGA-AMP and free ampicillin on the inhibition of MRSA, MSSA, and clinical strains' biofilm formation at 24, 48, and 72 hours are presented in Figures 5–7, respectively. Both PLGA-AMP and free ampicillin exhibited effectiveness in inhibiting biofilm formation at 24, 48, and 72 hours of incubation. Conversely, strains exposed to free PLGA and the positive control strains (untreated) displayed robust biofilm formation. During the 24- and 48-hour intervals, it was observed that free ampicillin exhibited a greater capacity to inhibit biofilm formation in all three strains when compared to PLGA-AMP. By the 72-hour time point, the impact of PLGA-AMP was significantly enhanced due to the gradual release of ampicillin. This led to PLGA-AMP achieving results that closely resembled those of free ampicillin, and, in some instances, even surpassing its efficacy. Nanoparticles that were conjugated with lysostaphin exhibited no discernible impact on the inhibition of biofilm formation during the 24, 48, and 72 hours of incubation. In these cases, the exposed strains continued to form strong biofilms.

Table 2: The PLGA-AMP formulation's technological features include average diameter, PDI, and zeta potential throughout the stability study (means ± SD, $n = 3$).

Formulation	Technological parameters	Time (months)					
		0	2	4	6	8	12
PLGA-AMP-LYS (F4)	Size (nm)	301.9 ± 32	304.3 ± 34	307.8 ± 32	312.5 ± 31	486.5 ± 36	502.6 ± 43
	PDI	0.261 ± 0.010	0.262 ± 0.014	0.264 ± 0.011	0.274 ± 0.017	0.278 ± 0.012	0.295 ± 0.016
	ZP* (mV)	−19.2 ± 3.4	−18.6 ± 3.2	−18.4 ± 2.2	−18.8 ± 4.6	−17.8 ± 3.8	−16.2 ± 4.3

*Zeta potential.

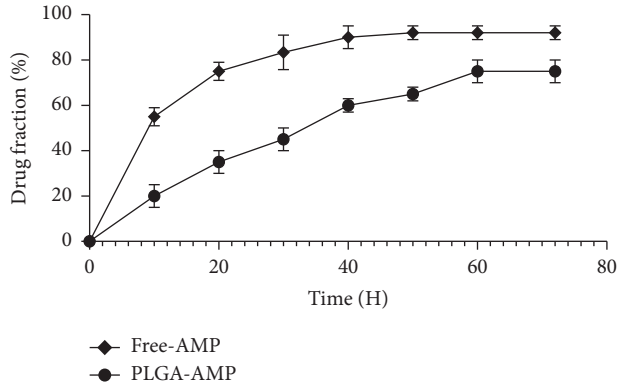

Figure 1: In a phosphate buffer with a pH of 7.4, the in vitro release profiles of ampicillin from the PLGA-AMP-LYS (F4) formulation were investigated. In this study, free ampicillin served as the control.

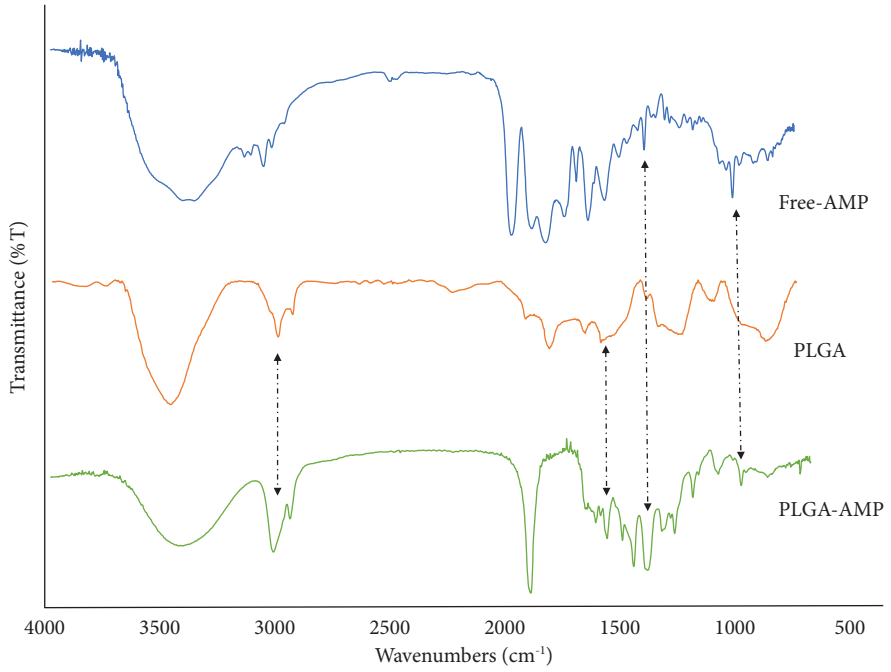

Figure 2: FTIR spectra of free-AMP, PLGA, and PLGA-AMP.

4. Discussion

Various methods are employed for drug loading within PLGA [7]. The synthesis method is chosen depending on the purpose of drug loading and preparation of the nanodrug and its important features. The present study utilized the double emulsion evaporation method to prepare nanodrugs. The findings showed that by using the mentioned method, the drug loading and encapsulation efficiency, zeta potential, PDI, size of the nanoparticles, and lysostaphin conjugation efficiency in the optimum PLGA-AMP-LYS (F4) formulation were 301.9 ± 32 nm, 0.261 ± 0.010, −19.2 ± 3.4 mV, 18.91 ± 1.6, and 94.53 ± 3.8, 40%, respectively. Considering the synthesized nanodrug's local use, the size was suitable.

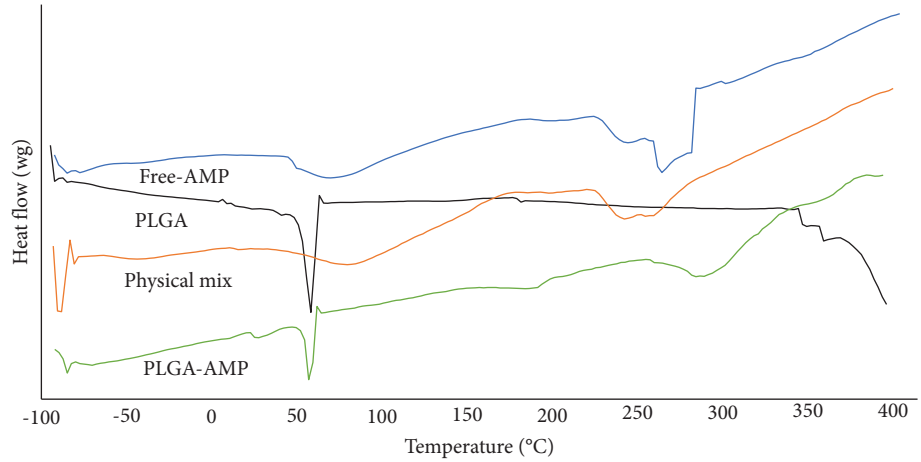

Figure 3: DSC thermograms of free-AMP, PLGA + free-AMP (physical mixture), PLGA, and PLGA-AMP.

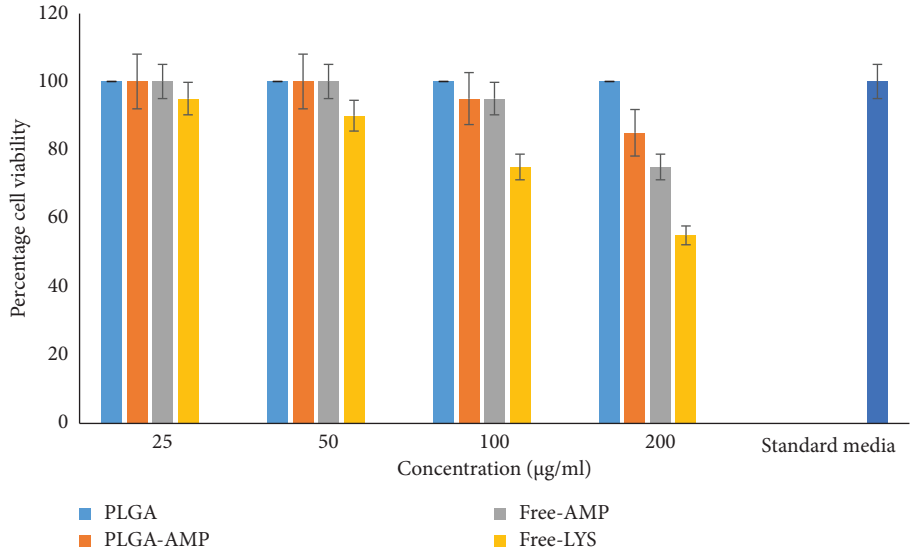

Figure 4: The PLGA-AMP, lysostaphin, and free-AMP effects on L929 cells.

Table 3: Results of MIC.

Time (h)	MIC value (μg/mL) 150-100-50-25-15-5-0.5 (μg/mL) Bacterial strains	PLGA-AMP	Free-AMP
24	MSSA	50 ± 4	5 ± 1
	MRSA	100 ± 7	50 ± 2
	Clinical strain	100 ± 5	15 ± 1
48	MSSA	25 ± 2	5 ± 1
	MRSA	100 ± 6	50 ± 5
	Clinical strain	50 ± 2	15 ± 1
72	MSSA	15 ± 1	5 ± 1
	MRSA	50 ± 5	50 ± 3
	Clinical strain	15 ± 1	30 ± 1

Furthermore, considering the zeta potential was −19.2 mV, the prepared nanodrug was stable. A rise in the negative zeta potential enhances particle stability by increasing repulsive forces, thereby preventing particle accumulation over time [39]. PVA is a surfactant and dispersing agent that affects nanoparticles' characteristics and reduces the surface tension between PLGA and water [39]. The important point was that while the amount of PVA in the synthesis process increased, the surface charge of the nanodrug increased, while the zeta potential became more negative. This finding aligns with the findings of Sharma et al. [40] because the surface charge of the nanodrug increased with the increment

Table 4: Results of agar well diffusion.

Time (h)	Bacterial strains	Zone of inhibition (mm) 50-25-5 (μg/mL) PLGA-AMP			Free-AMP		
24	MSSA	25	15	10	45	30	25
	MRSA	5	0	0	10	0	0
	Clinical strain	15	10	5	40	30	15
48	MSSA	30	20	15	45	30	25
	MRSA	10	5	0	10	0	0
	Clinical strain	20	15	5	40	30	15
72	MSSA	35	25	20	45	30	25
	MRSA	10	5	0	10	0	0
	Clinical strain	25	20	10	40	30	15

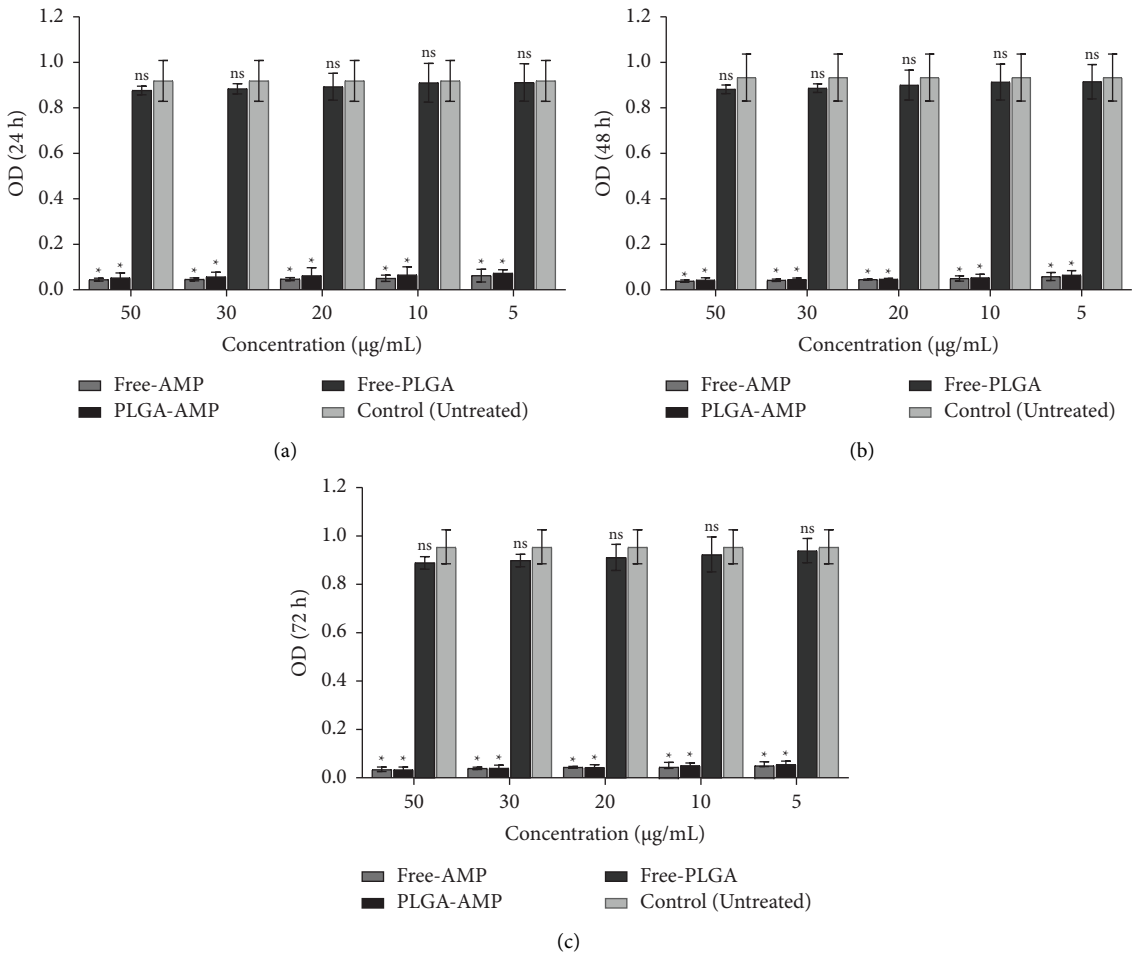

Figure 5: Graphical depiction of biofilm inhibition (OD values) of methicillin-resistant staphylococcus by different formulations in (a) 24, (b) 48, and (c) 72 hours. Comparisons were performed among free AMP, PLGA-AMP, free-PLGA, and control (treatment): NS, non-significant; $^{*}p < 0.05$.

of the surfactant amount in their study, which was a stabilizing agent and prevented the aggregation of nanoparticles and provided stability during the synthesis. Furthermore, in our investigation, the augmentation of PVA concentration resulted in a reduction in nanoparticle size, in line with the observations made by Hernández-Giottonini et al. [41]. They found that the nanoparticle size diminished as the PVA concentration increased, which they attributed to the increase in viscosity following the increase in PVA concentration. However, it should be mentioned that the majority of surfactants are toxic in nature, and their use is restricted. Fortunately, PVA has fewer toxic effects than other surfactants, such as tween, lecithin, and poloxamer; however, the optimum amount of PVA should be used. Another important factor in the synthesis of the nanodrug was the amount of PDI, which was 0.261. Many factors are

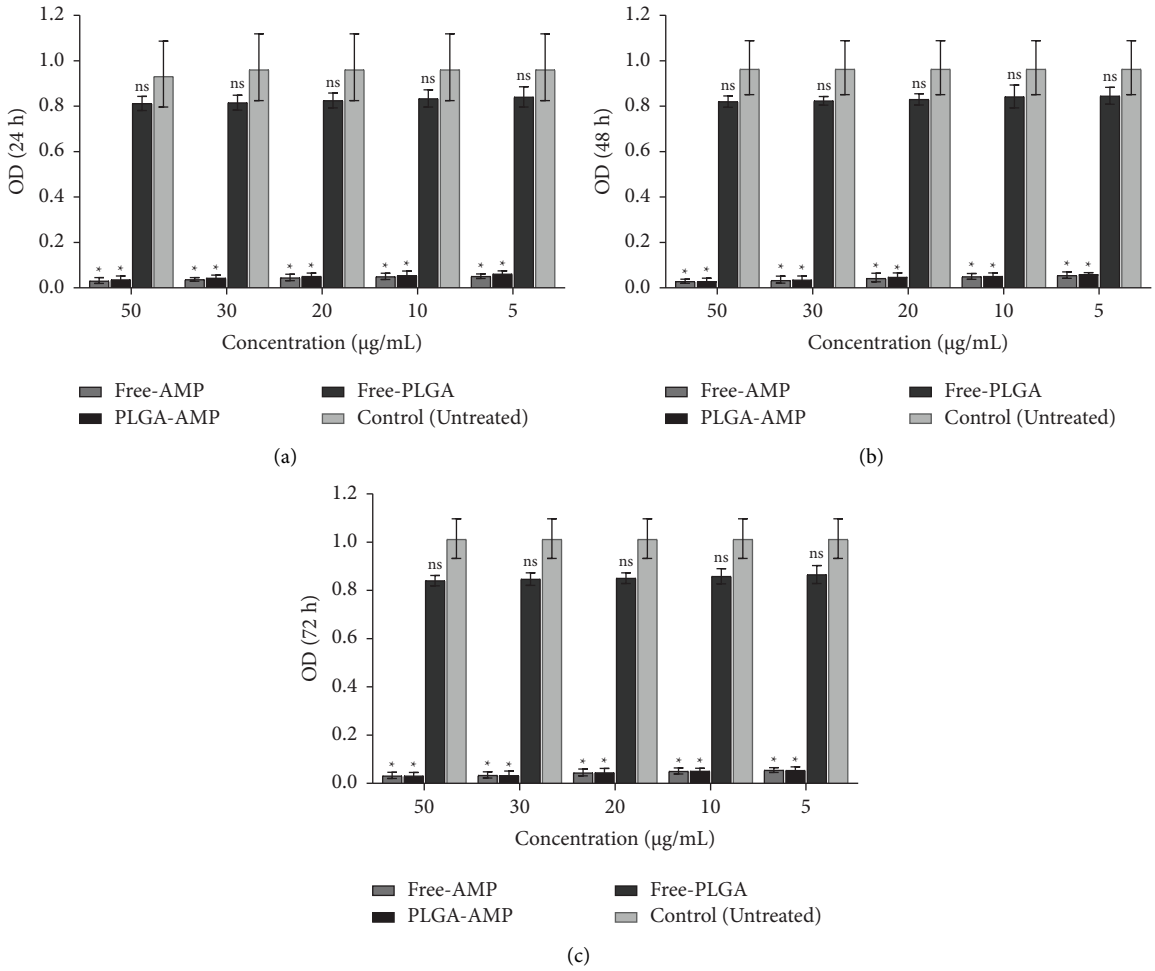

Figure 6: Graphical depiction of biofilm inhibition (OD values) of methicillin-sensitive staphylococcus by different formulations in (a) 24, (b) 48, and (c) 72 hours. Comparisons were performed among free AMP, PLGA-AMP, free-PLGA, and control (treatment): NS, non-significant; $^{*}p < 0.05$.

important in the PDI. For example, if we increase the duration of the ultrasonic probe during the synthesis, the particle size will decrease and become more homogeneous. As in our study, as the duration of using the magnetic stirrer increased, the PDI was smaller. However, is it possible to determine the size of PDI without considering the amount of load and encapsulation? Our findings showed that increasing the duration of using the ultrasonic probe and magnetic stirrer reduced drug loading and encapsulation amount, so a balance between the amount of loading and PDI should be achieved during the synthesis. This observation corresponds with the outcomes reported by Ito et al. [42]. In their study, it was found that the drug loading decreased as the homogenization time increased. Another important aim of this study was to determine the amount of drug loading in the PLGA matrix. The quantity of drug loading and encapsulation holds significant importance in enhancing the efficacy of therapeutic drugs, and it also warrants further investigation for their potential clinical applications [40]. In this current study, the drug loading and encapsulation levels in PLGA were assessed using the indirect spectrophotometer method, and drug absorption was measured at 268 nm wavelength. In our study, the drug loading was 18.91%, and the encapsulation efficiency was 94.53%. As the quantity of the drug was elevated, the drug loading capacity also increased, aligning with the findings reported by Snejdrova et al. [43]. In general, the drug loading capacity is contingent on multiple factors, such as the drug's characteristics (hydrophilic or hydrophobic), the synthesis method employed, and the quantity of the drug utilized [40, 44]. Besides, Sharma et al. [40] study revealed that the encapsulation rate of paclitaxel in PLGA was higher than that of epirubicin, which was attributed to the hydrophobic nature of paclitaxel, which easily interacts with the hydrophobic part of PLGA. Also, their study showed that surfactant concentration affected drug loading and nanoparticle encapsulation. As mentioned, the type of synthesis technique selected and the quantity of the drug directly impact the drug loading capacity. Wang et al. [45] loaded the natural compound paenol with the nanoprecipitation method, a suitable method for loading hydrophobic drugs, and the loading and encapsulation amounts in PLGA were 12.7% and 86%, respectively. The drug loading may be reduced due to the selection of an inappropriate synthesis method leading

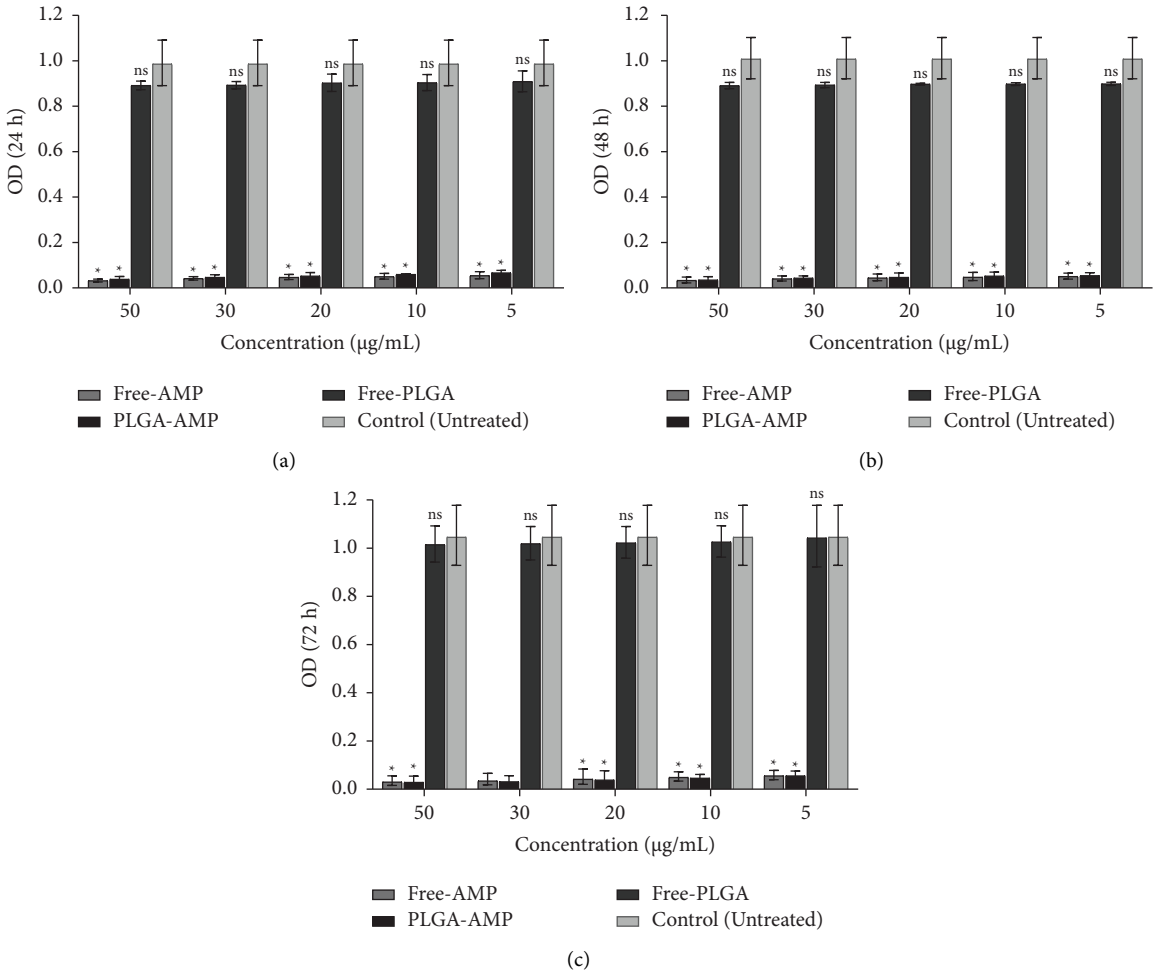

Figure 7: Biofilm inhibition (OD values) of staphylococcus by formulations shown graphically in (a) 24 hours, (b) 48 hours, and (c) 72 hours. The following comparisons were made: free AMP, PLGA-AMP, free-PLGA, and control (treatment): nonsignificant, or NS; $^{*}p < 0.05$.

to drug leakage outside the nanoparticle and drug destruction during the synthesis process [43]. Additionally, the kind of solvent used for PLGA during synthesis is a critical factor that influences the size, polydispersity index (PDI), and drug loading. In the present study, dichloromethane was first used as a solvent for PLGA. Nonetheless, due to inadequacies in terms of size, PDI, and drug loading, along with the low solubility of PLGA in dichloromethane, the synthesized nanoparticles were not considered suitable, so dichloromethane was replaced by chloroform. As a result, with the better solubility of PLGA in chloroform, the size and PDI decreased and drug loading also increased. Our findings were congruent with the study of Kim et al. [46], indicating that the solubility of PLGA in acetone was better than dichloromethane, and using dichloromethane during the synthesis of nanoparticles caused an increase in size and a lower encapsulation. For the reason that the duration of stability of nanoparticles is important, in our study, the stability of PLGA-AMP-LYS (F4) was investigated for 12 months. In the current investigation, notable alterations in size, PDI, and zeta potential were not observed for up to six months following the synthesis, while after 12 months of nanodrug preparation, PLGA-AMP size increased from 301.9 nm to 502.6 nm. This can be due to the adhesion of nanoparticles. However, there were no significant differences noted in zeta potential and PDI after the 12 months. Additionally, one of the advantages of the load of the drug in polymer nanoparticles is controlling the drug release rate following the polymer matrix's destruction, so the load of the drug in nanoparticles leads to a stable and controlled release of the drug in the desired region. Consequently, this enhances the drug's stability within the desired range [46]. The cross-linking of lactic acid and glycolic acid monomers with the drug gives rise to the creation of a polymer layer encasing the drug, facilitating a controlled and stable release of the drug from the nanoparticle [47]. In the current research, to investigate the release of ampicillin from PLGA-AMP-LYS (F4), the free drug and the nanodrug were enclosed inside two dialysis bags separately. Each one was located separately in a PBS medium (pH: 7.4). Our results demonstrated that, within 10 hours, approximately 55% of ampicillin was released from the dialysis bag into the release medium, while only 20% of ampicillin was released from the nanodrug during the same time. After 72 h, 92% of free ampicillin and

75% of ampicillin from the nanodrug were released in the release medium. The slow release of ampicillin from nanodrugs can be attributed to drug release from the nanoparticle core and the decomposition of PLGA into lactic acid and glycolic acid monomers [39]. However, the time it takes for drugs to be released from various types of nanoparticles can vary across different research studies, and one of the main reasons is the use of various materials and methods. Generally speaking, the extended drug release duration from nanoparticles compared to free drug results from the gradual release of the drug from the nanoparticle matrix. In the study of Zakeri-Milani et al. [39], initially, vancomycin exhibited a rapid release from PLGA, but over time, the rate of drug release from PLGA decreased. The rapid initial release of the drug was attributed to its presence on or near the surface of the PLGA, while the delayed release from the center of the PLGA was also noted. In our study, FE-SEM was used to examine the morphology of the synthesized nanoparticles. Electron microscopy results were consistent with PDI. Because according to Supplementary file 1, the particles' size was the same, with a smooth and spherical surface. The slight difference in nanoparticle diameter size in DLS and SEM results can be attributed to the fact that DLS determines the hydrodynamic diameter in solution, while SEM images are obtained without solvent [48]. Additionally, in the present study, the conjugation of lysostaphin on PLGA-AMP in the presence of NHS and EDC was created by creating a link between the carboxyl end of PLGA and the amine end of lysostaphin. The Bradford kit showed a 40% efficiency in lysostaphin conjugation. In Moura et al.'s study [26], the percentage of anti-CD46 conjugation on PLGA ranged from 31% to 36% in different formulations. On the other hand, FTIR and DSC were used in this investigation to verify that during the synthesis of PLGA-AMP, the elements did not chemically react with each other and were not converted into a new compound, and additionally to confirm that the drug was not physically located next to PLGA, and the results were completely promising. One of the most important topics in the synthesis and use of nanodrugs is the investigation of their toxicity. Due to the truth that the purpose of using nanomedicines is disease treatment in humans, investigating toxicity is of paramount significance. In the present study, PLGA-AMP at a 50 μg/ml concentration had no toxicity on L929 fibroblast cells, so 100% of the cells survived. Additionally, in our study, at a 200 μg/ml concentration, the toxicity of PLGA-AMP was lower than that of free ampicillin on cells. Therefore, drug encapsulation in nanoparticles may reduce toxicity. In the study of Liang et al. [49], the toxicity of rifapentine-loaded PLGA (RPT/PLGA NPs) on J744A.1 cell line was investigated. The survival of cells exposed to RPT/PLGA NPs at a 50 μg/mL concentration was above 90%, while the survival of cells exposed to free rifapentine at the same concentration was 40%. Their research demonstrated a substantial reduction in the toxicity of rifapentine following its encapsulation in PLGA. In our study, following the investigation of the synthesized nanoparticles' characteristics, well diffusion, MIC, and biofilm inhibition tests were performed to investigate their antimicrobial activity. Besides, 5, 25, and 50 μg/mL of free ampicillin were found more effective than PLGA-AMP on MRSA, MSSA, and clinical strains at 24 and 48 hours. But after 72 h, the size of the diameter of the halo of growth inhibition in the optimum formulation of PLGA-AMP and free ampicillin was almost the same. Since this method allows the bacteria to be in direct contact with the drug, the free ampicillin had a better effect in 24 and 48 h, while according to the release rate of the prepared nanodrug, which is 72 h, the halos became closer to each other during this time. Also, the MIC of free ampicillin at 24 and 48 h was lower than that of PLGA-AMP. However, after 72 h, the MIC of the optimum formulation of PLGA-AMP decreased due to the release of ampicillin from PLGA and approached the MIC of free ampicillin. Well diffusion and MIC study findings were predictable due to the long release time of PLGA-AMP. Free ampicillin was available from the start to exert its antimicrobial mechanism, while the drug was released from PLGA-AMP gradually. These findings align with the outcomes of Hosseini et al.'s study [31]. Additionally, our inquiry aimed at inhibiting the biofilm formation of *Staphylococcus aureus* strains. We investigated the effect of PLGA-AMP and free ampicillin on biofilm formation by MRSA, MSSA, and clinical strains. The results obtained after 72 h were promising. In all stages of the experiment, strains exposed to pure PLGA and the control group displayed robust biofilm formation, whereas those exposed to PLGA-AMP and free ampicillin exhibited diminished biofilm formation. At 24 and 48 h, a small amount of ampicillin was released from PLGA-AMP, so biofilm formation in all three bacterial strains was less inhibited than free ampicillin. While free ampicillin was completely in direct contact with bacteria and inhibited biofilm formation with a higher percentage than PLGA-AMP, biofilm formation was more affected by the increase in ampicillin release from PLGA-AMP after 72 h. The outcomes with PLGA-AMP were comparable to those with free ampicillin, and in certain instances, even slightly better, especially after 72 hours. According to Lange et al.'s study [50], Ag-NPs measuring 154 nm in size with a zeta potential of −26 mV exhibited a more pronounced impact on biofilm formation compared to Cu-NPs, which had a size of 345 nm and a zeta potential of −0.4. In their study, it is assumed that a more negative zeta potential leads to greater stability and the tendency of nanoparticles to accumulate is less, so their surface is not limited, and as a result, the antibacterial property is stronger. Also, smaller nanoparticles will penetrate deeper layers better. Also, in the study of Bastari et al. [51], levofloxacin was loaded in PLGA coated with calcium phosphate. Their study showed that both PLGA loaded with levofloxacin coated with calcium phosphate and uncoated prevented Staphylococcus aureus biofilm formation for four weeks. It is important in our study that the amount of ampicillin loading in PLGA-AMP before lysostaphin conjugation was 18.91%. Following the conjugation of lysostaphin, the researchers reevaluated well diffusion, MIC (minimum inhibitory concentration), and biofilm formation inhibition tests. Nanoparticles conjugated with lysostaphin had no antimicrobial and antibiofilm activity, while PLGA-AMP had antimicrobial and antibiofilm activity.

Therefore, we assume that drug release occurred during the conjugation of lysostaphin on PLGA-AMP because in the stage of lysostaphin conjugation, PLGA-AMP was dissolved in EDC and NHS and stirred for one hour. Next, in order to separate the precipitate of the nanodrug, centrifugation was performed. In the next step, lysostaphin was added to the precipitate of the nanodrug placed at 4°C for 24 hours and centrifuged. Therefore, the drug may have been removed from PLGA-AMP during this period.

5. Conclusion

In this study, a nanodrug was effectively synthesized using the double emulsion evaporation method, making it a potential treatment candidate for *Staphylococcus aureus* infections and the inhibition of biofilm formation by such strains. The antimicrobial effectiveness of free ampicillin surpassed that of PLGA-AMP in both the MIC and well diffusion assays at 24 and 48 hours, as ampicillin was released from PLGA-AMP over a span of approximately 72 hours. Consequently, the duration of effectiveness for PLGA-AMP in the well diffusion and MIC methods was 72 hours. Furthermore, in comparison to PLGA-AMP, free ampicillin exhibited a more pronounced impact on inhibiting the biofilm formation of *Staphylococcus aureus* strains. Nonetheless, their results showed remarkable consistency, and in certain cases, they exhibited even slight improvements after the 72 hour mark. Hence, the outcomes of our research highlight the promising efficacy of the optimal PLGA-AMP formulation after 72 hours. Utilizing this technology holds the potential to reduce staphylococcal infections and could serve as a valuable tool in managing hospital-acquired infections caused by this bacterium.

Data Availability

The datasets utilized and/or examined in the present study can be obtained from the corresponding author upon reasonable request.

Ethical Approval

This study received approval from the Ethics Committee of Hamadan University of Medical Sciences (Approval Code: IR.UMSHA.REC.1400.467).

Conflicts of Interest

The authors confirm the absence of any conflicts of interest.

Authors' Contributions

MRA, SMH, ENZ, and MASH were responsible for designing the study. EN, SMH, FK, and BA collaborated on the experimental work and contributed to drafting the manuscript. MRA, EN, and SMH conducted the data analysis. EN and SMH were involved in the cell culture, while SMH and RM were responsible for designing the nanoparticles. MRA oversaw the entire process, from design to review, and prepared the manuscript. All authors reviewed and approved the final manuscript.

Acknowledgments

The authors express their gratitude to the Hamadan University of Medical Sciences for its financial support in facilitating this research. Financial support for this study was provided by the Hamadan University of Medical Sciences under project no. 140007276055.

Supplementary Materials

Scanning electron microscopy of PLGA-AMP nanoparticles using field emission technology. (*Supplementary Materials*)

References

[1] S. Fulaz, H. Devlin, S. Vitale, L. Quinn, J. P. O'Gara, and E. Casey, "Tailoring nanoparticle-biofilm interactions to increase the efficacy of antimicrobial agents against *Staphylococcus aureus*," *International Journal of Nanomedicine*, vol. 15, pp. 4779–4791, 2020.

[2] A. Iannitelli, R. Grande, A. D. Stefano et al., "Potential antibacterial activity of carvacrol-loaded poly (DL-lactide-co-glycolide)(PLGA) nanoparticles against microbial biofilm," *International Journal of Molecular Sciences*, vol. 12, no. 8, pp. 5039–5051, 2011.

[3] H. Devlin, S. Fulaz, D. W. Hiebner, J. P. O'Gara, and E. Casey, "Enzyme-functionalized mesoporous silica nanoparticles to target *Staphylococcus aureus* and disperse biofilms," *International Journal of Nanomedicine*, vol. 16, pp. 1929–1942, 2021.

[4] N. Gómez-Sequeda, J. Ruiz, C. Ortiz, M. Urquiza, and R. Torres, "Potent and specific antibacterial activity against *Escherichia coli* O157: H7 and methicillin resistant *Staphylococcus aureus* (MRSA) of G17 and G19 peptides encapsulated into Poly-Lactic-Co-Glycolic Acid (PLGA) nanoparticles," *Antibiotics*, vol. 9, no. 7, p. 384, 2020.

[5] A. Shariati, Z. Chegini, E. Ghaznavi-Rad, E. N. Zare, and S. M. Hosseini, "PLGA-based nanoplatforms in drug delivery for inhibition and destruction of microbial biofilm," *Frontiers in Cellular and Infection Microbiology*, vol. 12, Article ID 926363, 2022.

[6] Z. Huang, T. Zhou, Y. Yuan et al., "Synthesis of carbon quantum dot-poly lactic-co-glycolic acid hybrid nanoparticles for chemo-photothermal therapy against bacterial biofilms," *Journal of Colloid and Interface Science*, vol. 577, pp. 66–74, 2020.

[7] H. K. Makadia and S. J. Siegel, "Poly lactic-co-glycolic acid (PLGA) as biodegradable controlled drug delivery carrier," *Polymers*, vol. 3, no. 3, pp. 1377–1397, 2011.

[8] J.-S. Choi, K. Seo, and J.-W. Yoo, "Recent advances in PLGA particulate systems for drug delivery," *Journal of Pharmaceutical Investigation*, vol. 42, no. 3, pp. 155–163, 2012.

[9] H. Ceotto-Vigoder, S. Marques, I. Santos et al., "Nisin and lysostaphin activity against preformed biofilm of *Staphylococcus aureus* involved in bovine mastitis," *Journal of Applied Microbiology*, vol. 121, no. 1, pp. 101–114, 2016.

[10] M. D. Bastos, B. G. Coutinho, and M. L. V. Coelho, "Lysostaphin: a staphylococcal bacteriolysin with potential clinical applications," *Pharmaceuticals*, vol. 3, no. 4, pp. 1139–1161, 2010.

[11] J. K. Kumar, "Lysostaphin: an antistaphylococcal agent," *Applied Microbiology and Biotechnology*, vol. 80, no. 4, pp. 555–561, 2008.

[12] S. Sharma, L. Singh, and S. Singh, "Comparative study between penicillin and ampicillin," *Scholars Journal of Applied Medical Sciences*, vol. 1, no. 4, pp. 291–294, 2013.

[13] J. Pazlarova, S. Purkrtova, J. Babulikova, and K. Demnerova, "Effects of ampicillin and vancomycin on *Staphylococcus aureus* biofilms," *Czech Journal of Food Sciences*, vol. 32, no. 2, pp. 137–144, 2014.

[14] J. L. Lister and A. R. Horswill, "*Staphylococcus aureus* biofilms: recent developments in biofilm dispersal," *Frontiers in Cellular and Infection Microbiology*, vol. 4, p. 178, 2014.

[15] P. Neopane, H. P. Nepal, R. Shrestha, O. Uehara, and Y. Abiko, "In vitro biofilm formation by *Staphylococcus aureus* isolated from wounds of hospital-admitted patients and their association with antimicrobial resistance," *International Journal of General Medicine*, vol. 11, pp. 25–32, 2018.

[16] M. Otto, "Community-associated MRSA: what makes them special?" *International Journal of Medical Microbiology*, vol. 303, no. 6-7, pp. 324–330, 2013.

[17] R. Parastan, M. Kargar, K. Solhjoo, and F. Kafilzadeh, "*Staphylococcus aureus* biofilms: structures, antibiotic resistance, inhibition, and vaccines," *Gene Reports*, vol. 20, Article ID 100739, 2020.

[18] N. K. Archer, M. J. Mazaitis, J. W. Costerton, J. G. Leid, M. E. Powers, and M. E. Shirtliff, "*Staphylococcus aureus* biofilms: properties, regulation, and roles in human disease," *Virulence*, vol. 2, no. 5, pp. 445–459, 2011.

[19] J. Liu, J.-Y. Madec, A. Bousquet-Mélou, M. Haenni, and A. A. Ferran, "Destruction of *Staphylococcus aureus* biofilms by combining an antibiotic with subtilisin A or calcium gluconate," *Scientific Reports*, vol. 11, no. 1, p. 6225, 2021.

[20] M. Otto, "Staphylococcal biofilms," *Microbiology Spectrum*, vol. 6, no. 4, pp. 6–4, 2018.

[21] K. M. Alarjani and M. Skalicky, "Antimicrobial resistance profile of *Staphylococcus aureus* and its in-vitro potential inhibition efficiency," *Journal of Infection and Public Health*, vol. 14, no. 12, pp. 1796–1801, 2021.

[22] G. Gebreyohannes, A. Nyerere, C. Bii, and D. B. Sbhatu, "Challenges of intervention, treatment, and antibiotic resistance of biofilm-forming microorganisms," *Heliyon*, vol. 5, no. 8, Article ID e02192, 2019.

[23] J. A. Wu, C. Kusuma, J. J. Mond, and J. F. Kokai-Kun, "Lysostaphin disrupts *Staphylococcus aureus* and Staphylococcus epidermidis biofilms on artificial surfaces," *Antimicrobial Agents and Chemotherapy*, vol. 47, no. 11, pp. 3407–3414, 2003.

[24] G. A. Hughes, "Nanostructure-mediated drug delivery," *Nanomedicine: Nanotechnology, Biology and Medicine*, vol. 1, no. 1, pp. 22–30, 2005.

[25] M. Yang, S. Xie, V. P. Adhikari, Y. Dong, Y. Du, and D. Li, "The synergistic fungicidal effect of low-frequency and low-intensity ultrasound with amphotericin B-loaded nanoparticles on C. albicans in vitro," *International Journal of Pharmaceutics*, vol. 542, no. 1-2, pp. 232–241, 2018.

[26] C. C. Moura, M. A. Segundo, J. D. Neves, S. Reis, and B. Sarmento, "Co-association of methotrexate and SPIONs into anti-CD64 antibody-conjugated PLGA nanoparticles for theranostic application," *International Journal of Nanomedicine*, vol. 9, pp. 4911–4922, 2014.

[27] P. Rafiei and A. Haddadi, "Docetaxel-loaded PLGA and PLGA-PEG nanoparticles for intravenous application: pharmacokinetics and biodistribution profile," *International Journal of Nanomedicine*, vol. 12, pp. 935–947, 2017.

[28] B. C. Garms, H. Poli, D. Baggley et al., "Evaluating the effect of synthesis, isolation, and characterisation variables on reported particle size and dispersity of drug loaded PLGA nanoparticles," *Materials Advances*, vol. 2, no. 17, pp. 5657–5671, 2021.

[29] A. Tripathi, R. Gupta, and S. A. Saraf, "PLGA nanoparticles of anti tubercular drug: drug loading and release studies of a water in-soluble drug," *International Journal of PharmTech Research*, vol. 2, no. 3, pp. 2116–2123, 2010.

[30] H. Chaudhary, H. Chaudhary, and V. Kumar, "Taguchi design for optimization and development of antibacterial drug-loaded PLGA nanoparticles," *International Journal of Biological Macromolecules*, vol. 64, pp. 99–105, 2014.

[31] S. M. Hosseini, R. Abbasalipourkabir, F. A. Jalilian et al., "Doxycycline-encapsulated solid lipid nanoparticles as promising tool against Brucella melitensis enclosed in macrophage: a pharmacodynamics study on J774A. 1 cell line," *Antimicrobial Resistance and Infection Control*, vol. 8, no. 1, pp. 62–12, 2019.

[32] T. S. J. Kashi, S. Eskandarion, M. Esfandyari-Manesh et al., "Improved drug loading and antibacterial activity of minocycline-loaded PLGA nanoparticles prepared by solid/oil/water ion pairing method," *International Journal of Nanomedicine*, vol. 7, pp. 221–234, 2012.

[33] M. Holgado, J. Arias, M. Cózar, J. Alvarez-Fuentes, A. Gañán-Calvo, and M. Fernández-Arévalo, "Synthesis of lidocaine-loaded PLGA microparticles by flow focusing: effects on drug loading and release properties," *International Journal of Pharmaceutics*, vol. 358, no. 1-2, pp. 27–35, 2008.

[34] K. K. Chereddy, R. Coco, P. B. Memvanga et al., "Combined effect of PLGA and curcumin on wound healing activity," *Journal of Controlled Release*, vol. 171, no. 2, pp. 208–215, 2013.

[35] Z. H. Wang, Z. Y. Wang, C. S. Sun, C. Y. Wang, T. Y. Jiang, and S. L. Wang, "Trimethylated chitosan-conjugated PLGA nanoparticles for the delivery of drugs to the brain," *Biomaterials*, vol. 31, no. 5, pp. 908–915, 2010.

[36] K. G. Bhat, T. M. Nalawade, and S. Sogi, "Antimicrobial activity of endodontic medicaments and vehicles using agar well diffusion method on facultative and obligate anaerobes," *International journal of clinical pediatric dentistry*, vol. 9, no. 4, pp. 335–341, 2016.

[37] P. Taylor, F. Schoenknecht, J. Sherris, and E. Linner, "Determination of minimum bactericidal concentrations of oxacillin for *Staphylococcus aureus*: influence and significance of technical factors," *Antimicrobial Agents and Chemotherapy*, vol. 23, no. 1, pp. 142–150, 1983.

[38] J.-H. Lee, Y.-G. Kim, and J. Lee, "Inhibition of *Staphylococcus aureus* biofilm formation and virulence factor production by petroselinic acid and other unsaturated C18 fatty acids," *Microbiology Spectrum*, vol. 10, no. 3, pp. e0133022–22, 2022.

[39] P. Zakeri-Milani, B. D. Loveymi, M. Jelvehgari, and H. Valizadeh, "The characteristics and improved intestinal permeability of vancomycin PLGA-nanoparticles as colloidal drug delivery system," *Colloids and Surfaces B: Biointerfaces*, vol. 103, pp. 174–181, 2013.

[40] N. Sharma, R. M. Kumari, N. Gupta, A. Syed, A. H. Bahkali, and S. Nimesh, "Poly-(lactic-co-glycolic) acid nanoparticles for synergistic delivery of epirubicin and paclitaxel to human lung cancer cells," *Molecules*, vol. 25, no. 18, p. 4243, 2020.

[41] K. Y. Hernández-Giottonini, R. J. Rodríguez-Córdova, C. A. Gutiérrez-Valenzuela et al., "PLGA nanoparticle

preparations by emulsification and nanoprecipitation techniques: effects of formulation parameters," *RSC Advances*, vol. 10, no. 8, pp. 4218–4231, 2020.

[42] F. Ito, H. Fujimori, and K. Makino, "Factors affecting the loading efficiency of water-soluble drugs in PLGA microspheres," *Colloids and Surfaces B: Biointerfaces*, vol. 61, no. 1, pp. 25–29, 2008.

[43] E. Snejdrova, J. Loskot, J. Martiska et al., "Rifampicin-loaded PLGA nanoparticles for local treatment of musculoskeletal infections: formulation and characterization," *Journal of Drug Delivery Science and Technology*, vol. 73, Article ID 103435, 2022.

[44] U. Posadowska, M. Brzychczy-Włoch, and E. Pamuła, "Gentamicin loaded PLGA nanoparticles as local drug delivery system for the osteomyelitis treatment," *Acta of Bioengineering and Biomechanics*, vol. 17, no. 3, pp. 41–48, 2015.

[45] F. Wang, Q. Shan, X. Chang, Z. Li, and S. Gui, "Paeonol-loaded PLGA nanoparticles as an oral drug delivery system: design, optimization and evaluation," *International Journal of Pharmaceutics*, vol. 602, Article ID 120617, 2021.

[46] D.-H. Kim, T. N. Nguyen, Y.-M. Han et al., "Local drug delivery using poly (lactic-co-glycolic acid) nanoparticles in thermosensitive gels for inner ear disease treatment," *Drug Delivery*, vol. 28, no. 1, pp. 2268–2277, 2021.

[47] H. Tang, J. Chen, L. Wang et al., "Co-delivery of epirubicin and paclitaxel using an estrone-targeted PEGylated liposomal nanoparticle for breast cancer," *International Journal of Pharmaceutics*, vol. 573, Article ID 118806, 2020.

[48] H. Bao, Q. Zhang, and Z. Yan, "The impact of camptothecin-encapsulated poly (lactic-co-glycolic acid) nanoparticles on the activity of cytochrome P450 in vitro," *International Journal of Nanomedicine*, vol. 14, pp. 383–391, 2019.

[49] Q. Liang, H. Xiang, X. Li et al., "Development of rifapentine-loaded PLGA-based nanoparticles: in vitro characterisation and in vivo study in mice," *International Journal of Nanomedicine*, vol. 15, pp. 7491–7507, 2020.

[50] A. Lange, A. Grzenia, M. Wierzbicki et al., "Silver and copper nanoparticles inhibit biofilm formation by mastitis pathogens," *Animals*, vol. 11, no. 7, p. 1884, 2021.

[51] K. Bastari, M. Arshath, Z. H. M. Ng et al., "A controlled release of antibiotics from calcium phosphate-coated poly (lactic-co-glycolic acid) particles and their in vitro efficacy against *Staphylococcus aureus* biofilm," *Journal of Materials Science: Materials in Medicine*, vol. 25, no. 3, pp. 747–757, 2014.